

consequently, the magnitude of β_X is increased as indeed observed experimentally.⁹ We should note here that the effect of nucleophile (X) on k_b is always much smaller than on k_{-a} and/or k_a .

As we increase the electron-donating power of RY (which can be expressed as $\delta\sigma_Y < 0$ if Y is considered as a substituent on the substrate), TS2 is stabilized more and bond cleavage is facilitated so that the Hammett coefficient of the leaving group, ρ_Z (ρ_{lg}) increases $\delta\rho_Z > 0$. Thus $\partial\rho_Z/\partial\rho_Y (= \rho_{YZ}) < 0$.¹¹ The negative sign of ρ_{YZ} is therefore a necessary condition for the rate-limiting breakdown of T^- .^{11b} This is of course true only in the gas-phase, in solution solvent effect can change the mechanism to a concerted one.

The lowering of pK_0 due to an electron-donating RY(CH₃ versus H) is a consequence of this negative ρ_{YZ} , since an electron-donating RY, $\delta\rho_Y < 0$, leads to an increase in bond cleavage, $\delta\rho_Z > 0$, which brings down the pK_0 point to a lower pK_a than that expected from a more electron-withdrawing RY group. This is what we obtained theoretically in this work on the gas-phase reactions of MNPA.

Acknowledgment. We thank the Inha University and the Korea Research Center for Theoretical Physics and Chemistry for support of this work.

References

1. Determination of Reactivity by MO Theory, Part 93. Part 92. Kim, C. K.; Chung, D. S.; Chung, K. H.; Lee, B.-S.; Lee, I. *J. Phys. Org. Chem.* In press.
2. (a) Bond, P. M.; Castro, E. A.; Moodie, R. B. *J. Chem. Soc., Perkin Trans. 2*, **1976**, 68. (b) Gresser, M. J.; Jencks, W. P. *J. Am. Chem. Soc.* **1977**, *99*, 6963, 6970. (c) Castro, E. A.; Freudenberg, M. *J. Org. Chem.* **1980**, *45*, 906. (d) Castro, E. A.; Steinfert, G. B. *J. Chem. Soc., Perkin Trans. 2*, **1983**, 453. (e) Castro, E. A.; Santander, C. L. *J. Org. Chem.* **1985**, *50*, 3595. (f) Castro, E. A.; Ureta, C. *J. Org. Chem.* **1989**, *54*, 2153. **1990**, *55*, 1676. (g) Castro, E. A.; Ureta, C. *J. Chem. Soc., Perkin Trans. 2*, **1991**, 63. (h) Castro, E. A.; Ibanez, F.; Saitua, A. M.; Santes, J. G. *J. Chem. Res.* **1993**, (S) 56 ; (M) 0317-0327.
3. (a) Ba-Saif, S.; Luthra, A. K.; Williams, A. *J. Am. Chem. Soc.* **1987**, *109*, 6362. (b) Ba-Saif, S.; Luthra, A. K.; Williams, A. *J. Am. Chem. Soc.* **1989**, *111*, 2647.
4. (a) Stefanidis, D.; Cho, S.; Dhe-Paganon, S.; Jencks, W. P. *J. Am. Chem. Soc.* **1993**, *115*, 1650.
5. Park, Y. S.; Kim, C. K.; Lee, B.-S.; Lee, I.; Lim, W. M.; Kim, W. K. *J. Phys. Org. Chem.* Submitted for publication.
6. Stewart, J. J. P. *J. comput. Chem.* **1989**, *10*, 221.
7. Csizmadia, I. G. *Theory and Practice of MO calculations on Organic Molecules*; Elsevier, Amsterdam, 1976, p 239.
8. (a) Jencks, W. P. *Chem. Soc. Rev.* **1981**, *10*, 354. (b) Williams, A. *Chem. Soc. Rev.* **1994**, *23*, 93.
9. Koh, H. J.; Lee, H. C.; Lee, H. W.; Lee, I. Submitted for publication.
10. (a) Pross, A. *Adv. Phys. Org. Chem.* **1997**, *14*, 69. (b) Johnson, C. D. *Chem. Rev.* **1975**, *75*, 755. (c) Melennan, D. *J. Tetrahedron.* **1978**, *34*, 2331. (d) Buncl, E.; Wilson, H. J. *Chem. Educ.* **1987**, *64*, 475. (e) Exner, O. *J. Chem. Soc., Perkin Trans. 2*, **1993**, 973.
11. (a) Lee, I. *Adv. Phys. Org. Chem.* **1992**, *27*, 57. (b) Lee, I. *Bull. Korean. Chem. Soc.* In press.

Photodissociation Dynamics of H₂O₂ at 280-290 nm

Sun Jong Baek, Seung Keun Shin, Chan Ryang Park[†], and Hong Lae Kim*

Department of Chemistry, College of Natural Sciences, Kangwon National University, Chuncheon 200-701, Korea

[†]*Department of Chemistry, College of Natural Sciences, Kookmin University, Seoul 136-702, Korea*

Received December 1, 1994

Laser induced fluorescence spectra of OH produced from photodissociation of H₂O₂ at 280-290 nm in the gas phase have been observed. By analyzing the Doppler profiles, the anisotropy parameter ($\beta = -0.7$) and the center of mass translational energy of the fragments have been measured. The measured energy distribution is well described by an impulsive model. The excited state leading to dissociation is found to be of ¹A_u symmetry. The dissociation from this state is prompt and direct with the fragment OH rotating in the plane perpendicular to the O-O bond axis.

Introduction

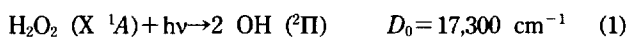
Doppler profiles in absorption or emission spectra of molecules in a chemically or photochemically changing system can provide valuable information on the dynamics of the process. In order to study the dynamics of such a process, it requires measurements of certain physical properties of the system such as energy distribution, angular distribution of

the final products, and so forth. Especially, vector properties such as recoil velocities and angular momenta of the final products are of great importance. These can be measured by translational spectroscopy using molecular beams and a mass spectrometer. However, in certain circumstances that the molecules or atoms in the system can absorb or emit radiation of an easily accessible spectral region, not only the energies distributed among quantum states of the product

molecules but also correlations between the vector properties of the system can be measured by analyzing the Doppler profiles of the spectra. Recently, this technique of Doppler spectroscopy has extensively been applied to study the dynamics of photodissociation,¹ although it has yet been applied very few to bimolecular reactions.^{2,3}

In Doppler spectroscopy, it is the most important that the molecules of interest should have high enough speed to show broad profiles to be measured correctly under the given spectral resolution. In this sense, OH from photodissociation of H₂O₂ is a very good candidate. It has been known that in the photodissociation of H₂O₂ in UV, the electronic absorption brings the parent molecule to a repulsive part of potential energy surfaces and therefore, most of the available energy may be transformed into the translational energy of the OH products. This should produce the Doppler profiles in the spectra of OH wide enough to be measured by laser induced fluorescence (LIF) under the present resolution of 0.12 cm⁻¹ of our dye laser.

The photodissociation of H₂O₂ in UV



has extensively been studied at several wavelengths and the vector as well as scalar properties of the system have been measured.⁴⁻⁷ It has been found that the transition dipole moment of the parent molecule at 266 nm lies parallel to the C₂ symmetry axis of the parent molecule (perpendicular transition) while at 193 and 248 nm the absorption shows the mixed transition, both perpendicular and parallel. At these excitation energies ab initio calculations predict several excited potential energy surfaces of different symmetries⁸ and it is important to find out the region of these surfaces from which the dissociation originates to understand the dynamics of the process in detail.

The correlation between the transition dipole moment, μ and the recoil direction of the product OH, v is very interesting because this can be measured by analyzing the Doppler profiles of the LIF spectra of OH. Since the absorption should take place with the maximum strength when the electric vector of the polarized dissociating light ϵ_d is parallel to the transition dipole moment, v and ϵ_d (and μ) should have definite correlations if the lifetime of the excited parent molecule is short enough compared to its rotational period. The correlation is described by

$$f(\theta_{v,\epsilon}) = [1/(4\pi)][1 + \beta P_2(\cos \theta_{v,\epsilon})] \quad (2)$$

where β is the anisotropy parameter which provides the angular distribution of the recoiling fragments ranging from 2 for the parallel ($\mu \parallel v$) to -1 for the perpendicular transition ($\mu \perp v$) and P_2 is the second order Legendre function. As a result, the Doppler profile of the spectra shows distinct shapes according to the types of the transition and the experimentally determined geometries.

Another important correlation is the correlation between the recoil velocity and the rotational angular momentum J of the fragments.⁹ While the μ, ϵ - v correlation produces the distinct shape in the Doppler profiles under the certain experimental geometries, this v - J correlation which is made upon the instance of dissociation should provide the characteristic line shapes by itself. When the fragments are probed

in the Q-branch rovibronic transition which has the maximum absorption for the transition dipole moment of the fragment parallel to J in the classical limit, and if v is also parallel to J (out-of-plane dissociation), the profile shows a maximum at the center. On the other hand, when the fragments are probed in the P and R-branches, the profile shows a minimum at the center in this case. By changing the experimental geometries, all these vector properties can be measured by analyzing the Doppler profiles of the spectra.

In this report, the Doppler profiles of the LIF spectra of OH produced from the photodissociation of H₂O₂ at 280-290 nm have been measured. The symmetry of the excited state leading to dissociation and the dynamics of the process have been discussed from the measured profiles and the energy distribution.

Experiment

The experiment was performed in a conventional flow cell made of stainless steel cube of 9 cm wide on which entrance and exit arms of 30 cm long are placed with two Brewster angle quartz windows at the end of both arms, respectively. The pressure inside the cell was maintained about 10⁻³ Torr with a liquid nitrogen trap and a mechanical pump. The gaseous sample was continuously flowed through the cell keeping the sample pressure of about 40 mTorr.

An output of a dye laser (Lumonics HD500) pumped by the second harmonic of a pulsed Nd:YAG laser (Lumonics YM800) was frequency doubled in a KDP crystal and used to dissociate H₂O₂. The pulse duration of this light is about 8 ns. Another photon of the same energy within the same pulse was subsequently absorbed by the fragment OH and induced the fluorescence. The R-branch bandhead of the rovibronic, $v=1 \leftarrow 0$, $^2\Sigma \leftarrow ^2\Pi$ transition of OH starts from around 281 nm and extends to the red. The absorption by H₂O₂ in UV is continuous starting from around 300 nm. The absorption cross section is on the order of 10⁻²⁰ cm² and is relatively constant in the region of 280-300 nm where the OH LIF spectra are measured.¹⁰ The linewidth of the dye laser output in the visible was measured from the linewidth of the LIF spectra of gaseous iodine, which was 0.06 cm⁻¹ and thus the linewidth of the doubled output in UV was at least 0.12 cm⁻¹. Laser induced fluorescence was measured through a bandpass filter which was centered at 320 ± 20 nm where the induced emission arising from the $v=1 \leftarrow 1$, $^2\Pi \leftarrow ^2\Sigma$ transition of OH transmitted. Baffles in both arms and various cut-off filters were used to minimize the scattered radiation. The fluorescence was monitored by a PMT (Hamamatsu R212U) and the signal was gated-integrated by a boxcar, digitized (EG & G 4420), and stored in a PC.

Under the above condition, nascent rotational distribution of the OH fragments could be measured. Signal intensities of various transitions from P, Q, and R-branches were measured as a function of the laser power. The graph showed straight lines of slope of 1.5 to 2.5 for the laser power of between 20 μJ/pulse and about 2 mJ/pulse, which suggests that this should be the two photon process, one photon dissociation and a subsequent photon probe. The laser power was maintained about 50 μJ/pulse to ensure that the spectra were measured without saturation.

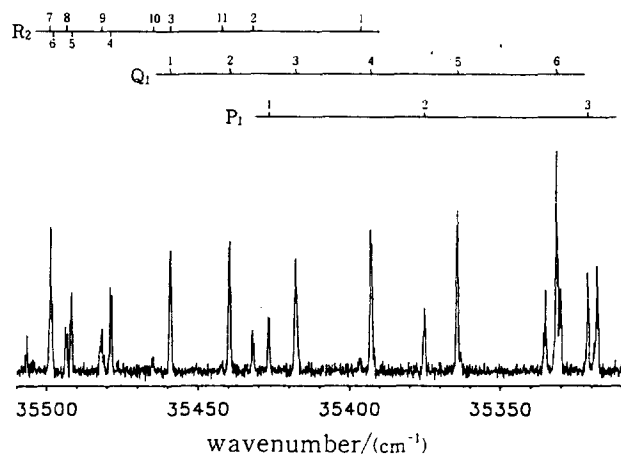


Figure 1. Portion of the LIF spectra of OH produced from photodissociation of H_2O_2 employing the $v=1\leftarrow 0$, ${}^2\Sigma\leftarrow{}^2\Pi$ electronic transition. Assignments of the rotational transitions are on top of the peaks.

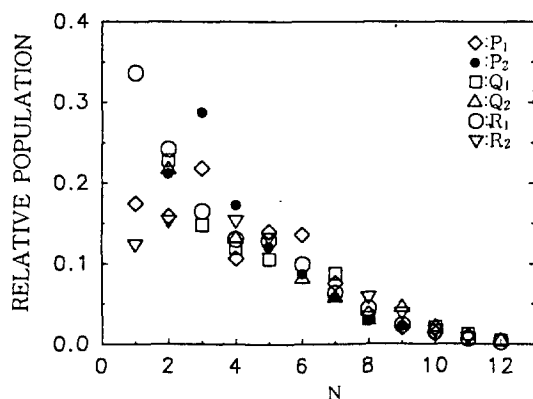


Figure 2. Relative rotational population distribution in both the ${}^2\Pi_{1/2}$ and ${}^2\Pi_{3/2}$ states of the OH fragments.

Results

LIF spectra of OH produced from the photodissociation at 280–290 nm employing the $v=1\leftarrow 0$, ${}^2\Sigma\leftarrow{}^2\Pi$ electronic transition have been measured and rotational transitions are assigned according to Dieke and Crosswhite.¹¹ Figure 1 shows a portion of the spectra with the assignments on top of the peaks. Intensities of the measured rotational transitions peak around $N=2$ and extend to $N=13$. Relative population distribution over rotational levels are measured with the reported Einstein B coefficients,¹² which is presented in Figure 2. From the distribution an average rotational energy of OH has been found to be about 700 cm^{-1} .

Doppler profiles of each rotational transition have been measured under high resolution. Typical profiles are in Figure 3 for $P_1(4)$ and $Q_1(10)$ where the linewidth of our laser is shown under the profile. The angular distribution described by (2) becomes

$$f(\theta_{z,v}) = [1/(4\pi)] [1 + \beta P_2(\cos \theta_{z,e}) P_2(\cos \theta_{z,v})] \quad (3)$$

using the Legendre polynomial theorem where the probe laser light propagates in the z direction. The fragment mov-

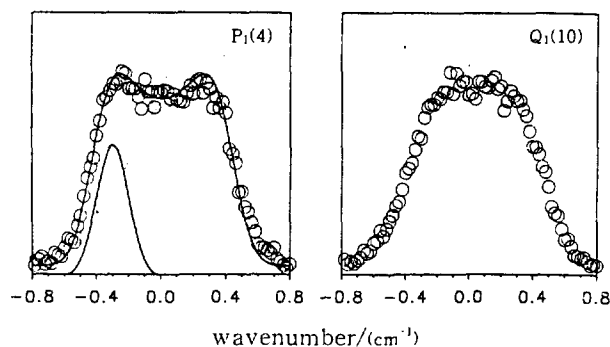


Figure 3. Typical Doppler profiles of the LIF spectra of OH measured under high resolution (circles). The laser lineshape is presented under the measured profile. The solid curve is the simulated profile by the equation (5) with $\beta = -0.7$ and $v = 3600\text{ ms}^{-1}$.

ing with a single velocity $v_z = v \cos \theta_{z,v}$ towards the observer absorbs light at a frequency $\nu = \nu_0(1 + v_z/c)$ where $\theta_{z,v}$ is the angle between the velocity of the fragment and the direction of the probing light and c is the speed of light. ν_0 is the absorption frequency of the fragment at rest. The distribution described above then provides the Doppler profiles given by

$$I(\nu) = [1/(4\pi)] [1 + \beta P_2(\cos \theta_{z,e}) \{3/2[(\nu - \nu_0)/\nu_0]^2 (c/v)^2 - 1/2\}]. \quad (4)$$

In our experiment, since the pump and probe light come from the same source, the ϵ vector of the dissociating light is perpendicular to the z direction which results in $P_2(\cos \theta_{z,e}, \epsilon) = -1/2$. Therefore, the final Doppler profiles should become

$$I(\nu) = [1/(4\pi)] [(1 - \beta/2) \{3/2[(\nu - \nu_0)/\nu_0]^2 (c/v)^2 - 1/2\}]. \quad (5)$$

The experimentally observed profiles have been simulated by (5) with the convolution of our laser lineshape changing the anisotropy parameter β and the speed of the fragment v assuming that the observed fragment should have a single speed. The best fits for the P and R -branch transitions have been obtained with $\beta = -0.7$ and $v = 3600\text{ ms}^{-1}$ and are represented as the solid lines in Figure 3. Since the speed of the fragment should have a distribution corresponding to the distribution of the internal energies of the other sibling fragment, the measured profile should be simulated with another convolution of the speed distribution. However, the observed internal energy distribution is so narrow that the measured speed from the simulation may represent the upper limit which is not expected to be far from the average speed. The transition leading to dissociation should be perpendicular that is, the transition dipole moment should lie parallel to the C_2 symmetry axis. However, for the Q -branch transitions, the measured profiles can not be reproduced with any β and v values. It suggests that there should be another correlation which determines the characteristic lineshapes of the Q -branch transitions. In fact, Gericke and co-workers found the slightly positive v - J correlations in 266 nm photodissociation which should produce the similar Doppler profiles observed in our experiment.⁶ If there is a positive v - J correlation, observed profiles should have higher

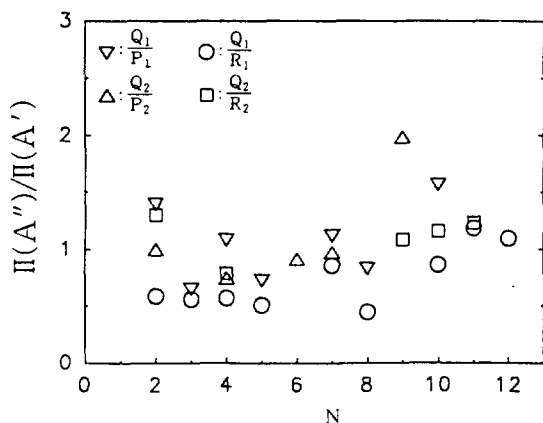


Figure 4. Λ -doublet distribution, $\Pi(A'')/\Pi(A')$ measured in both the ${}^2\Pi_{1/2}$ and ${}^2\Pi_{3/2}$ states of the OH fragments.

intensity in the Q-branch transitions than in the P- and R-branch transitions at the center, and if there is a negative v - J correlation, the observed profiles should show a reverse trend. In our experiment it is impossible to measure such a correlation quantitatively because we should have at least two different experimental geometries. However, the anisotropy parameter and the qualitative nature of the v - J correlation can be obtained from the simulation fitted to the experimentally observed profiles. Center of mass translational energy of the system measured from the speed of OH is 18,600 cm^{-1} .

Coupling of rotational and electronic orbital angular momenta produces two Λ -doublet fine structure states.¹³ In diatomic molecules with half filled π electrons such as in OH, electronic wavefunction of the unpaired electron is, in the limit of high rotation, approximated to the atomic orbital wavefunction which has definite symmetries with respect to the plane of molecular rotation. The symmetric wavefunction represented as a lobe in the plane of rotation is assigned to the A' state among the two Λ -doublet components while the antisymmetric wavefunction as a lobe perpendicular to the plane is assigned to the A'' state. These definite parities form rotational selection rules in electronic transitions such as the P- and R-branch transitions should be induced from the A' state and the Q-branch transitions from the A'' state. The Λ -doublet distribution measured from the Q and P, R-branch transitions in both the ${}^2\Pi_{3/2}$ and ${}^2\Pi_{1/2}$ electronic states shows a slight propensity in the A'' state as N increases (Figure 4). If there is no preference of the population in the two Λ -doublet states, the ratio should be unity. Since the observed ratio $\Pi(A'')/\Pi(A')$ is slightly larger than the unity at high N , the atomic orbitals for the unpaired electron in the OH fragments formed from the photodissociation are expected to lie perpendicular to the plane of molecular rotation of OH.

Discussion

Photodissociation dynamics of polyatomic molecules is governed by the potential energy surfaces where the molecules reach by the absorption of light. *Ab initio* calculation of the electronic structure of H₂O₂ predicts several low-lying exci-

ted states in the region of 280-290 nm excitation which correlate to both the OH fragments in the ground state, ${}^2\Pi$. By using a simple molecular orbital description, the lowest energy excited state electronic configuration is

$$A \ {}^1A_u: \cdots(4a_g)^2(5a_u)^2(4b_g)^1(5b_u)^1 \quad (6)$$

with 3 Π' and 3 Π'' electrons. Another low-lying excited state is

$$B \ {}^1B_g: \cdots(4a_g)^2(5a_u)^1(4b_g)^2(5b_u)^1. \quad (7)$$

The next higher lying C state can be reached by the excitation of two nonbonding electrons to the antibonding molecular orbital, which requires much higher energy. In the transition from the ground electronic state $X \ {}^1A_g$ to A 1A_u state, the transition dipole moment of the parent H₂O₂ molecule should lie perpendicular to the O-O bond whereas to the B 1B_g state, the transition dipole moment should lie parallel to the O-O bond. The measured anisotropy parameter $\beta = -0.7$ without any v - J correlation shows that the transition dipole moment is perpendicular to the O-O bond. Therefore, it can be concluded that the absorption of the light at 280-290 nm by H₂O₂ brings the molecule to the excited state of 1A_u symmetry. The anisotropy parameter β has the limiting value of -1 for the perpendicular transition. The deviation of the measured $\beta = -0.7$ from the limiting value is mainly due to the rotation of the parent molecule during the dissociation. The correlation between the molecular rotational period and the β value has been reported by Yang and Bersohn.¹⁴ The average rotational period of H₂O₂ along the C axis at ambient temperature is about 10 ps. From the measured β value, the lifetime of the excited H₂O₂ molecule is expected to be shorter than the rotational period of the parent molecule.

Dissociation of H₂O₂ from the strongly repulsive A state is expected to be instantaneous and direct judging from the measured anisotropy parameter. This prompt photodissociation is often described by an impulsive model.¹⁵ A very steep repulsive potential is created between the O-O atoms in H₂O₂ upon excitation followed by a sharp recoil of the O atoms releasing their repulsive potential energy over such a short distance that the O-H bond length and the angle $\angle\text{OOH}$ are scarcely changed upon separation of the O atoms. At this point the energy available in O-O repulsion, E_{av} , is partitioned by conservation of linear momentum between the kinetic energies of the two O atoms which in turn are partitioned between translation, rotation, and vibration of OH when the recoiling O atoms collide with H. If the parent H₂O₂ is stationary in the beginning, the total translational energy of the fragments is

$$E_t(\text{OH}) = \frac{\mu(\text{O-O})}{\mu(\text{OH-OH})} E_{av} = 0.94 E_{av} \quad (8)$$

where μ 's are the reduced mass of the atoms at the end of the breaking bond and the reduced mass of the fragments, respectively. The impulse between the two O atoms exerts a torque on OH resulting in the fragment rotation in the plane of O-O-H. Since the angular momenta of the two OH fragments are cancelled each other, the rotational energy of the OH fragment is given by

$$E_r(\text{OH}) = \left[1 - \frac{\mu(\text{O-O})}{\mu(\text{OH-OH})} \right] \sin^2 \gamma \quad E_{av} = 0.06 E_{av} \quad (9)$$

where γ is the angle, $\angle \text{OOH}$ ($=98.5^\circ$).

The total available energy which is the photon energy (for example at 282 nm $h\nu=35,460 \text{ cm}^{-1}$) and the average internal energy of the parent molecule ($E_v + E_r \approx 400 \text{ cm}^{-1}$ at ambient temperature) subtracted by the dissociation energy ($17,300 \text{ cm}^{-1}$) is $18,560 \text{ cm}^{-1}$. The fractions of the measured center of mass translational energy and rotational energy are 0.97 and 0.03 of the total available energy, respectively. Although the measured translational energy may be overestimated in the convolution procedure, the translational and rotational energies are reasonably well described by the impulsive model.

The fragment rotation may originate from either the internal motion of the parent molecule or the torque developed upon dissociation. Even though the impulsive model well describes the measured rotational energy, a portion of the rotational energy should come from the parent internal motion. Among the six vibrational modes of H_2O_2 the ν_4 torsional mode is the lowest frequency fundamental. This torsional motion is well described by an internal rotation. Indeed the excited potential function of the A state strongly depends upon the torsional angle which shows a minimum at the trans-planar configuration of H_2O_2 while the ground state potential has a local maximum at this configuration.¹⁶ However, the barrier is so low that the initial internal rotational levels are significantly populated and upon excitation this torsional energy is transformed into OH rotation.

The electronic configuration of the A state predicts the population among the two Λ -doublet states of the fragment OH to be equal unless there is any dynamical process involved in dissociation. However, as seen in Figure 3 the Doppler profiles of the Q and P-branch transitions suggest that there should be a v - J correlation. In 266 nm photodissociation, a slightly positive v - J correlation has been observed, which shows the rotational angular momentum vector J is parallel to the recoil direction v : the fragment OH rotates in the plane perpendicular to v and J .⁵ This out-of-plane dissociation is also expected from the fragment rotation which originates from the parent torsional motion. Since the unpaired p orbital in the fragment OH is formed upon breaking the O-O bond, it tends to lie along the O-O bond axis which is the recoil direction of the fragment. As a result, in the high J limit, the $\Pi(A'')$ Λ -doublet component would be more populated than the (A') component. On the other hand, if the fragment rotation originates solely from the torque by

the impulse between the separating two O atoms in the plane, the $\Pi(A')$ component of the Λ -doublet should be more populated. Although the Λ -doublet distribution is easily scrambled by the parent rotation,¹⁷ the measured distribution in this experiment shows a slight propensity in $\Pi(A'')$, which supports the out-of-plane dissociation.

In summary, the photodissociation of H_2O_2 at 280-290 nm is prompt and direct with the fragment OH rotating in the plane perpendicular to the O-O bond axis (out-of-plane dissociation). The excited state leading to dissociation is of 1A_u symmetry and the dissociation is well explained by the impulsive model.

Acknowledgment. This work was supported by the Korea Science and Engineering Foundation (92-26-00-01).

References

1. *Molecular Photodissociation Dynamics*; ed. by Ashfold, M. N. R.; Baggott, J. E. Royal Society of Chemistry, London, 1987.
2. Brouard, M.; Duxon, S. P.; Enriquez, P. A.; Simons, J. *P. J. Chem. Phys.* **1992**, *97*, 7414.
3. Kim, H. L.; Wickramaaratchi, M. A.; Zheng, X.; Hall, G. E. *J. Chem. Phys.* **1994**, *101*, 2033.
4. Ondrey, G.; Van Veen, N.; Bersohn, R. *J. Chem. Phys.* **1983**, *78*, 3732.
5. Vaghjiani, G. L.; Ravishankara, A. R. *J. Chem. Phys.* **1990**, *92*, 996.
6. Gericke, K.-H.; Klee, S.; Comes, F. J.; Dixon, R. N. J. *Chem. Phys.* **1986**, *85*, 4463.
7. Klee, S.; Gericke, K.-H.; Comes, F. J. *Ber. Bunsenges. Phys. Chem.* **1988**, *92*, 429.
8. Chevaldonnet, C.; Cardy, H.; Dargelos, A. *Chem. Phys.* **1986**, *102*, 55.
9. Houston, P. J. *J. Phys. Chem.* **1987**, *91*, 5388.
10. *Photochemistry of Small Molecules*; Okabe, H. John Wiley & Sons: New York, 1978.
11. Dieke, G. H.; Crosswhite, H. M. *J. Quant. Spectrosc. Radiat. Transfer*, **1962**, *2*, 97.
12. Chidsey, I. L.; Crosley, D. R. *J. Quant. Spectrosc. Radiat. Transfer*, **1980**, *23*, 187.
13. Hanazaki, I. *Chem. Phys. Lett.* **1993**, *201*, 301.
14. Yang, S.-C.; Bersohn, R. *J. Chem. Phys.* **1974**, *61*, 4400.
15. Busch, G. E.; Wilson, K. R. *J. Chem. Phys.* **1972**, *56*, 3626.
16. Block, R.; Jansen, L. *J. Chem. Phys.* **1985**, *82*, 3322.
17. Andresen, P.; Rothe, E. W. *J. Chem. Phys.* **1985**, *82*, 3634.